JOURNAL OF Materials CHEMISTRY

C_{60} in the box. A supramolecular C_{60}–porphyrin assembly

Dirk M. Guldi,*[a] Tatiana Da Ros,[b] Paolo Braiuca,[b] Maurizio Prato*[b] and Enzo Alessio*[c]

[a] *Radiation Laboratory, University of Notre Dame, Notre Dame, IN 46556, USA. E-mail: guldi.1@nd.edu*
[b] *Dipartimento di Scienze Farmaceutiche, Università di Trieste, Piazzale Europa, 1, 34127 Trieste, Italy. E-mail: prato@univ.trieste.it*
[c] *Dipartimento di Scienze Chimiche, Università di Trieste, Italy. E-mail: alessi@univ.trieste.it*

Received 28th February 2002, Accepted 2nd April 2002
First published as an Advance Article on the web 9th May 2002

A novel supramolecular complex with C_{60} in a porphyrin box has been computer-modeled using a docking program. The same complex has been experimentally studied by means of time-resolved spectroscopy and compared with another porphyrin box characterized by a different geometry. The results show that rapid singlet energy transfer occurs in toluene — the product of a very effective intermolecular interaction — only when the geometry allows C_{60} to fit into the box, whereas no interaction was detected when access to the box was physically denied.

Introduction

Supramolecular architectures, in which photo-/electroactive donors and acceptors are preorganized intermolecularly *via* non-covalent linkages, are particularly appealing since they might provide long-lived charge separated states.[1] In essence, in such weakly-bonded systems, a rapid photoinduced electron transfer (ET) should be followed by a splitting of the charge separated components, thus mimicking a key step in photosynthesis.[2] Therefore, the development of synthetic strategies aimed at associating a donor and an acceptor in a well-defined geometry through non-covalent linkages is a current issue of high interest.[3] Besides, the weak molecular interactions offer an opportunity to control (*i*) the organization of photo- and redox active components and (*ii*) their mutual, electronic coupling. A better understanding of how the separation, mutual orientation, and electronic coupling between donor and acceptor affect the rates and yields of energy and electron transfer reactions is expected to facilitate and, ultimately, allow the tuning of such processes.[4]

In principle, a variety of non-covalent interactions, such as hydrogen-bond, donor–acceptor complexation, electrostatic interactions and π–π stacking, can be exploited for the design and synthesis of donor–acceptor systems with high directionality and selectivity for achieving predetermined architectures.[5]

A fascinating scenario involves the utilization of strong π–π interactions between metalloporphyrins (MP) and C_{60} to engineer supramolecular arrays with remarkable photophysical and magnetic properties.[6] This aspect has been systematically explored in a series of MP/C_{60} cocrystallites with M being Mn, Co, Ni, Cu, Zn and Fe. Favorable van der Waals attractions between the curved π-surface of C_{60} and the planar π-surface of MP assist in the supramolecular recognition, despite the geometrical mismatch between the concave-shaped host and the convex-shaped guest structure. This leads to complexes with unusually short contact distances (2.7–3.0 Å), shorter than ordinary van der Waals separations (3.0–3.5 Å), and a variety of crystal structures, ranging from zig-zag chains to columns.[6b]

Attractive van der Waals forces between porphyrins and C_{60} are also appreciable in condensed media, constituting an important organizational principle.[7,8] Importantly, whenever allowed by the molecular topology of the system, these moieties spontaneously tend to achieve close spatial proximity relative to each other. To ensure strong association constants in combination with well-defined geometries, we have adopted a multi-point contact approach, in which C_{60} interacts with a self-assembled porphyrin box **ZnP(4)-(RuP)$_4$** (**1**).[9] The box is formed by four side wall ruthenium porphyrins, RuP, axially connected through Ru-pyridine coordination bonds to one central zinc 4′-tetrapyridylporphyrin, ZnP(4). We show that this system is useful for exploiting the supramolecular interactions of the porphyrin systems with the fullerene acceptor at the molecular level. A comparison with the more compact pentamer box **ZnP(3)-(RuP)$_4$** (**2**) (obtained using 3′-tetrapyridylporphyrin, ZnP(3), instead of ZnP(4)), in which the side-wall RuP groups are tilted rather than orthogonal to the central ZnP, will also be described.

Results and discussion

Synthesis and modeling

The chemical structures of the compounds studied herein are shown in Schemes 1–3.[9]

The structure of the porphyrin box (**1**) was initially minimized by simple molecular mechanics. The geometry of fullerene C_{60} was optimized using the semiempirical PM3 method (see Experimental Section for details). The two structures were docked together, in order to obtain the most stable relative orientation. The final complex had a stabilization energy of 10.6 kcal mol^{-1} and is reported in Fig. 1. The C_{60} sphere finds its position in the center of the porphyrin box, 3 Å from the Zn atom (*i.e.*, distance from the closest carbon atom in C_{60}) and about 6.5 Å from the side phenyl rings, thus forming a highly symmetrical complex.

The structure of the isomeric box (**2**) is based on its X-ray structure and its three-dimensional image was generated using Sybyl 6.8 program on a Silicon Graphics workstation (Fig. 2).

Photochemistry

Photochemistry of ZnP and RuP references. The emission properties of the **ZnP** (**3**) and **RuP** (**4**) references can be summarized as follows: only **ZnP** (**3**) fluoresces ($E_{singlet}$ = 2.05 eV) strongly with an overall quantum yield of 0.04, for which we determined a radiative lifetime of 2.3 ns in

DOI: 10.1039/b202116a

This journal is © The Royal Society of Chemistry 2002

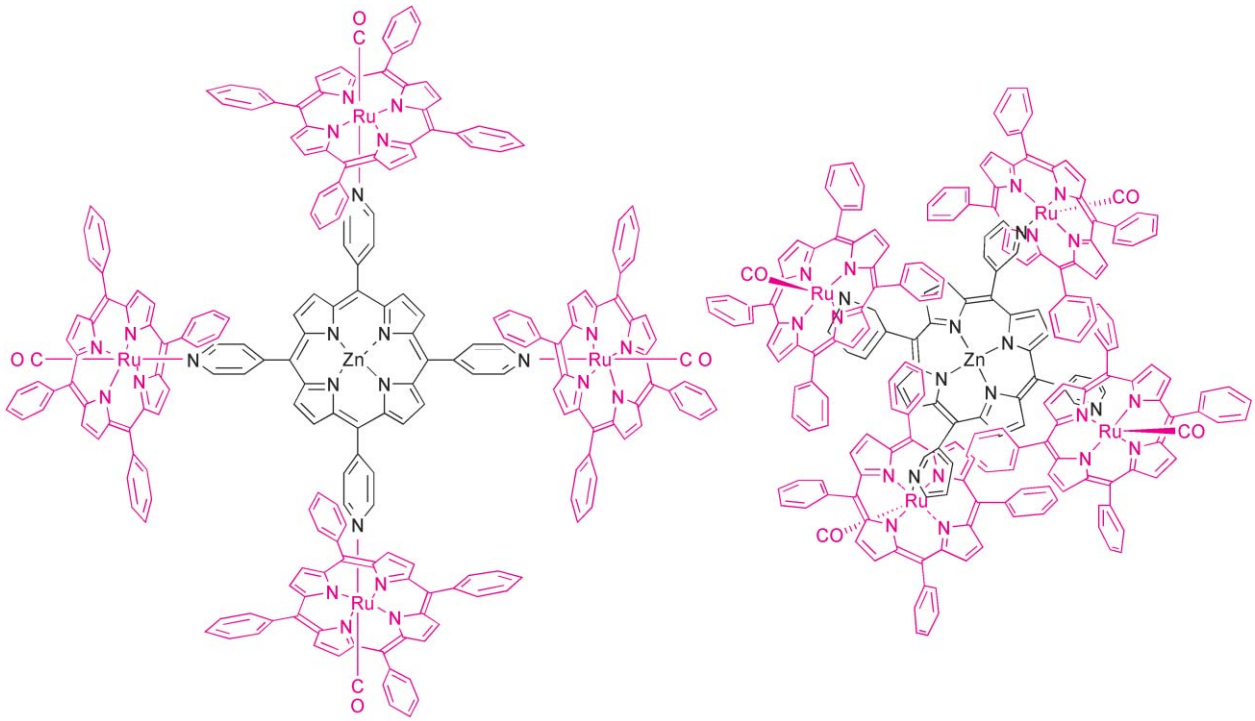

Scheme 1

deoxygenated toluene. In contrast, the heavy-atom effect (see below) present — induced by the ruthenium metal — eliminates any detectable singlet excited state emission in the corresponding **RuP** (**4**) complex ($E_{singlet}$ = 2.2 eV).

Just the opposite trend emerges for the phosphorescence features. In particular, **RuP** (**4**) was found to be the only reference compound to show measurable room temperature phosphorescence with a quantum yield of *ca.* 10^{-3} and a triplet energy ($E_{triplet}$) of 1.68 eV. Lowering the temperature to 77 K helped in activating the moderate triplet excited state emission of **ZnP** (**3**) ($E_{triplet}$ = 1.53 eV). Noteworthy, in both cases, phosphorescence shows high sensitivity to the presence of oxygen, with participation in *inter*molecular energy transfer reactions (*vide infra*).

As far as transient absorption spectroscopy is concerned, 18 ps excitation of the **ZnP** (**3**) reference led to characteristic absorption changes in the region between 400 and 810 nm. A net decrease of the absorption was observed in regions that are dominated by strong **ZnP** (**3**) ground state transitions, for example, by the S_0–S_2 *Soret*-band (*i.e.*, 420 nm) and S_0–S_1 *Q*-band (*i.e.*, 550 nm). This suggests consumption of **ZnP** (**3**) as a result of converting the porphyrin singlet ground state to the corresponding singlet excited state, ^{1}*(π–π*)ZnP. A concomitantly formed absorption in the red — between 550 and 650 nm — accompanies this bleaching. Both singlet excited state features — transient absorption and bleaching — correspond to a singlet lifetime of 2.5 ± 0.2 ns. The singlet excited state converts predominantly (~88%) to the triplet manifold, ^{3}*(π–π*)ZnP. Differential absorption changes of the latter state reveal dominant peaks in the visible (λ_{max} = 380 and 470 nm) and also a characteristic fingerprint in the near-infrared (λ_{max} = 860 nm). As an illustration, the 860 nm transition is displayed in Fig. 3.

In a strictly oxygen-free environment (*i.e.*, toluene) the triplet

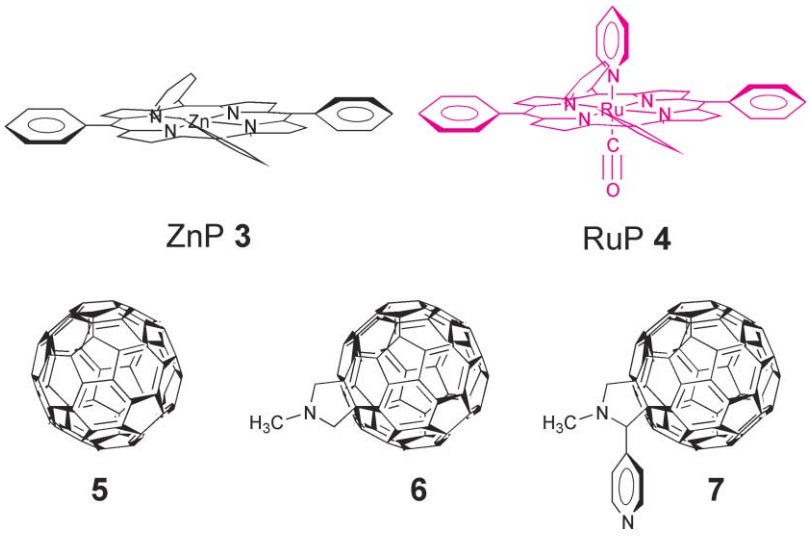

Scheme 2

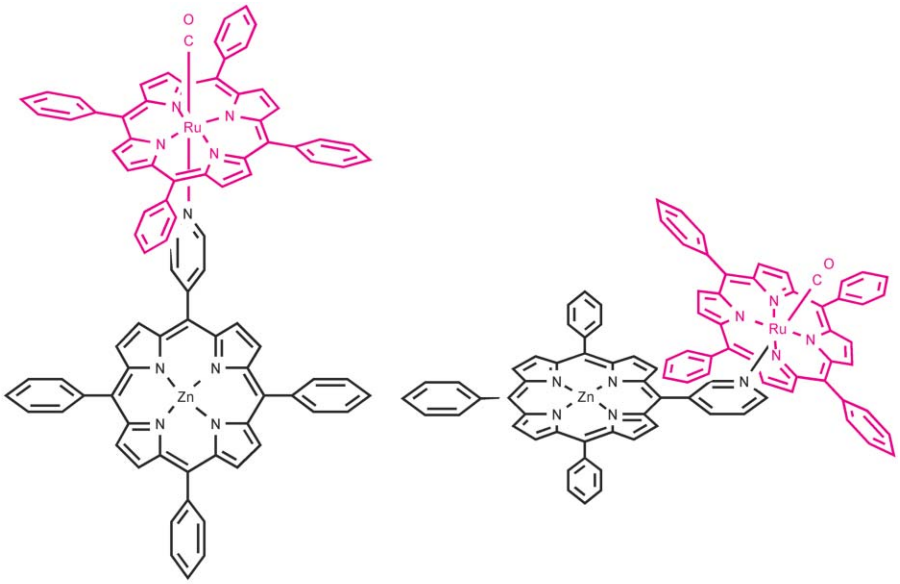

Scheme 3

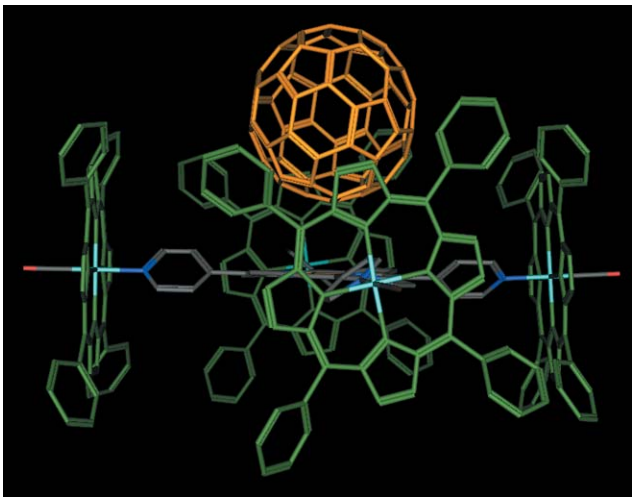

Fig. 1 Docked image of C_{60} in **ZnP(4)-RuP$_4$** (**1**).

excited state decayed with clean first-order kinetics, restoring the singlet ground state. A triplet lifetime of 44 μs was deduced from the maxima in the visible and red.

Quite different is the situation for the analogous **RuP** (**4**). Relative to the **ZnP** (**3**) analogue, the heavy nucleus of the ruthenium metal leads to a much stronger spin-orbit coupling. The latter is responsible for the instantaneous, spin-forbidden transformation of the singlet to the triplet excited state. This

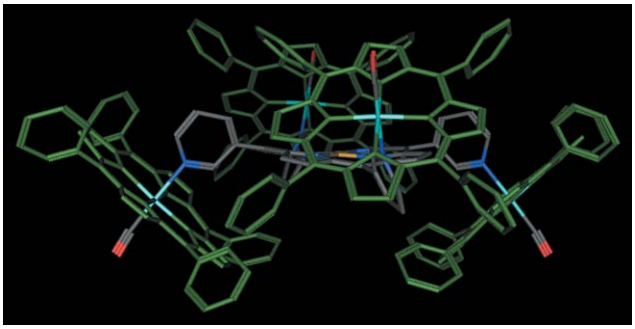

Fig. 2 Crystallographic structure of **ZnP(3)-RuP$_4$** (**2**).

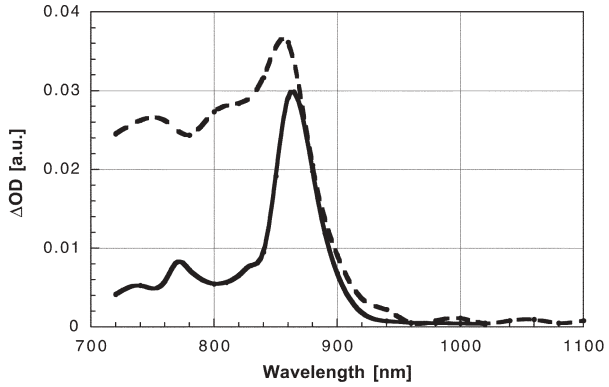

Fig. 3 Nanosecond transient absorption spectrum (near-infrared part) recorded at 50 ns upon flash photolysis of **ZnP** (**3**) (2×10^{-5} M) (dashed line) and **RuP** (**4**) (2×10^{-5} M) (solid line) at 532 nm in deoxygenated toluene.

leads to the conclusion that the lifetime of the initially formed ^{1}*(π–π*)RuP must lie out of our detection range (*i.e.*, < 18 ps). Accordingly, the differential absorption changes, recorded immediately after the laser pulse, with maxima at 370, 470, 580 and 870 nm (Fig. 3) are attributes of the ^{3}*(π–π*)RuP. This state shows no appreciable deactivation and only complementary flash photolysis experiments in the nano- and microsecond regime allowed us to determine a lifetime of 30 μs for the **RuP** (**4**) triplet excited state, slightly shorter than what was seen for **ZnP** (**3**), 44 μs.

The triplet quantum yields in these reference porphyrins were determined as 0.88 and 0.65 for **ZnP** (**3**) and **RuP** (**4**), respectively and, in turn, underline their efficient population. Upon admitting a triplet quencher, such as molecular oxygen, to the porphyrin solutions, the triplet excited states of both porphyrins experience a marked acceleration of their triplet decays. These truly *inter*molecular reactions involve the photosensitization of cytotoxic singlet oxygen, as independently confirmed by the corresponding ($^1\Delta_g$) O_2 phosphorescence at 1270 nm. We probed for this assay oxygen concentration varying between 0.9 and 9.8 mM, which led generally to faster decays of the triplet features. Importantly, the observed rates ($k_{obs} = \ln 2/\tau_{1/2}$) were linearly dependent on the oxygen concentration. From the slopes of the k_{obs} *versus* [O_2]

plots, *inter*molecular rate constants of 6.5×10^8 $M^{-1}s^{-1}$ and 7.1×10^8 $M^{-1}s^{-1}$ were determined for the reaction between molecular oxygen and ^{3}*(π–π*)ZnP or ^{3}*(π–π*)RuP, respectively. Moreover, oxygen saturated conditions (*i.e.*, 9.8×10^{-3} M in toluene) led to singlet oxygen quantum yields of 0.76 (**3**) and 0.63 (**4**).

Photochemistry of C_{60} (1) and fulleropyrrolidine (2) reference. The photophysical behavior of C_{60} (**5**) and fulleropyrrolidine (**6**) has been the subject of a number of reviews and is in principle well understood.[10] Therefore, we wish only to highlight the most fundamental photophysical parameters of these references.

In terms of radiative processes, a weakly fluorescent singlet excited state (quantum yields for **5**: 2×10^{-4}; **6**: 6×10^{-4}) with excited state energies of 1.99 eV (**5**) and 1.76 eV (**6**) transforms with an almost unitary quantum yield into an energetically low-lying triplet excited state ($\sim$1.5 eV). The latter state emits even weaker than the former with a barely detectable phosphorescence quantum yield on the order of 10^{-6}.

The transient absorption associated with the singlet excited state of **5** and **6** discloses characteristic singlet–singlet transitions at around 920 nm ($\varepsilon \sim 7000$ M^{-1} cm^{-1}) and 890 nm ($\varepsilon \sim 10000$ M^{-1} cm^{-1}), respectively. A large spin-orbit coupling, stemming predominantly from the fullerene curvature, promotes the fast intersystem crossing dynamics found in **5** and **6** with time constants of nearly 5.0×10^8 s^{-1}. This leads consequently to the C_{60} triplet excited state. In the context of the current investigation, the most important absorption feature of these triplet states is a strong maximum in the visible region at 750 nm ($\varepsilon = 20000$ M^{-1} cm^{-1}) and 700 nm ($\varepsilon = 16000$ M^{-1} cm^{-1}) for **5** and **6**, respectively — summarized in Fig. 4.

Under ambient conditions, triplet lifetimes of C_{60} and C_{60} derivatives are generally quite short, since they are strongly effected by a variety of annihilation processes, ranging from triplet–triplet to triplet–ground-state quenching. Under our standard experimental conditions, namely, a nitrogen-purged toluene solution containing tens of micromolar concentrations of **5** or **6**, lifetimes typically of about 25 μs are found.

Photochemistry of ZnP(4)-RuP (8) and ZnP(3)-RuP (9) references. The two ZnP-RuP dimers, orthogonal **ZnP(4)-RuP** (**8**) and canted **ZnP(3)-RuP** (**9**), and their intrinsic ZnP-RuP linkages represent the basic motifs in box (**1**) and box (**2**), respectively. Thus, they emerged as useful references, fostering our understanding of the more complex porphyrin boxes.

As far as the ^{1}*(π–π*)ZnP fluorescence (Fig. 5a; λ_{exc} at 550 nm, which corresponds to the *Q*-band maximum of the **ZnP** (**3**) ground state absorption) is probed, somewhat affected

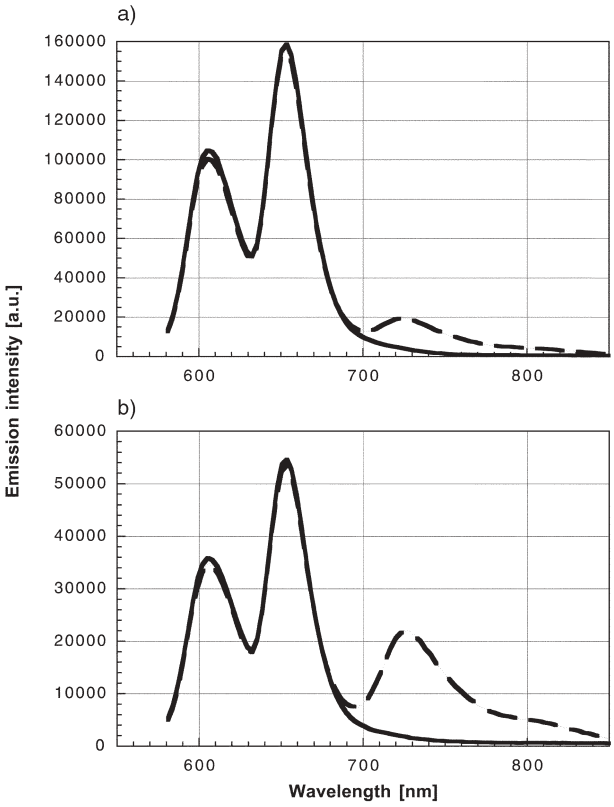

Fig. 5 Emission spectra of **ZnP(4)-RuP** (**8**) (2×10^{-5} M) (a) λ_{exc} = 550 nm — maximum of the ZnP ground state absorption in deoxygenated (solid line) and oxygenated (dashed line) toluene solutions and (b) λ_{exc} = 532 nm — maximum of the RuP ground state absorption in deoxygenated (solid line) and oxygenated (dashed line) toluene at room temperature.

quantum yields ($\Phi = 0.015$) and lifetimes ($\tau = 0.89$ ns, Fig. 6) in (**8**), led us to assume some electronic interactions with the ruthenium center. An *intra*molecular transduction of singlet excited state energy is thermodynamically implausible, since it implicates an uphill reaction by about 0.15 eV. Consequently, this leaves a faster intersystem crossing rate, imposed by the RuP spin-orbit perturbation, as the only likely cause. This phenomenon is amplified with increasing the number of RuP groups, as demonstrated below for (**1**) and (**2**).

At room temperature, the steady-state phosphorescence of dimers (**8**) and (**9**) reveal a strongly quenched ^{3}*(π–π*)RuP emission with 16% and 15% of that seen for the **RuP** (**4**) reference (Fig. 5b; λ_{exc} at 532 nm, which corresponds to the *Q*-band maximum of the **RuP** (**4**) ground state absorption). After

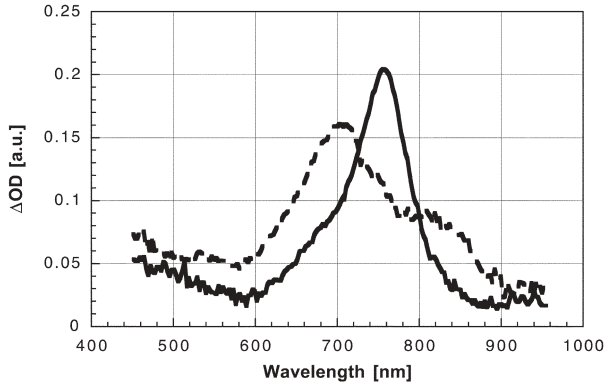

Fig. 4 Nanosecond transient absorption spectrum (visible-near-infrared part) recorded at 50 ns upon flash photolysis of **5** (5×10^{-5} M) (solid line) and **6** (5×10^{-5} M) (dashed line) at 532 nm in deoxygenated toluene.

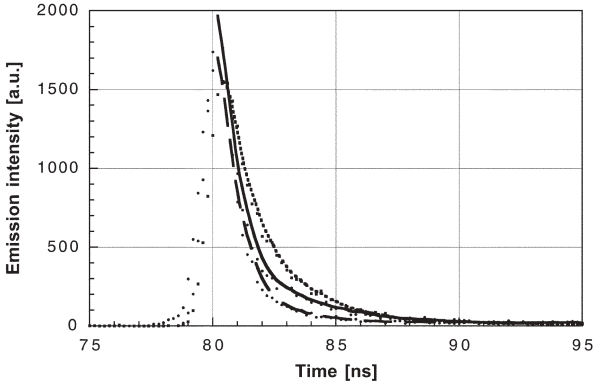

Fig. 6 Time-resolved fluorescence decay of (**8**) (2×10^{-5} M) (dotted line) and of (**1**) (2×10^{-5} M)(solid line) as monitored in toluene at the 600 nm emission maximum and scatterer (dashed line). Laser excitation was at 337 nm.

examining the energetics of the states involved, the most conceivable rationale for this quenching appears to be a fast, *intra*-molecular triplet–triplet energy transfer from the ^{3}*(π–π*)RuP (1.68 eV) to the energetically lower lying ^{3}*(π–π*)ZnP (1.53 eV).[11] A similar trend emerged from the phosphorescence decay measurements at the 725 nm maximum. Lifetimes of 545 ps (**8**) and 233 ps (**9**) attest to the rapid deactivation of ^{3}*(π–π*)RuP.

Due to the weak emission of the ZnP triplet state, at least, in room temperature experiments, we employed transient absorption spectroscopy to gather spectroscopic evidence in support for the energy transfer pathway. Excitation of both dimers with a short 532 nm laser pulse leads to the instantaneous bleaching of the RuP *Q*-band absorption centered around 535 nm, while the wavelength region above 570 nm is dominated by the strong absorption of the excited state with maxima at 580 and 870 nm (see Fig. 7 at the 25 ps time delay). All these features are in excellent agreement with those linked to the triplet excited state of **RuP** (**4**). But instead of the slow regeneration of the singlet ground state, these characteristics transform rather rapidly into a broadly absorbing species. In particular, lifetimes of 284 ps and 486 ps were derived for (**9**) and (**8**), respectively, which are in excellent agreement with the fluorescence lifetimes. The spectrum of the new transient, which is identical for both dimeric porphyrin systems, shows a minimum at 550 nm, a broad transition between 550 and 650 nm (Fig. 7; at 1000 ps time delay) and a maximum at 860 nm and is an excellent match of the triplet excited state of **ZnP** (**3**), namely, ^{3}*(π–π*)ZnP (see for comparison Fig. 3). Moreover the derived lifetime of *ca.* 27 μs differs only marginally from that measured for **ZnP** (**3**). Additional evidence for the proposed energy transfer route is given by the high quantum yield (~70%) of ^{3}*(π–π*)ZnP formation, as concluded from the 860 nm absorption.

Photochemistry of ZnP(4)-(RuP)$_4$ (1) and ZnP(3)-(RuP)$_4$ (2) boxes. The lowest lying excited state in both porphyrin boxes, (**1**) and (**2**), is — similar to the energetics summarized for the (**8**) and (**9**) dimers — the triplet excited state of the central ZnP with a triplet energy of 1.53 eV.

Regarding the emission of the ZnP and RuP moieties in (**1**) and (**2**) we would like to emphasize several important observations. First, it is notable that the ZnP fluorescence remains further affected by the presence of the surrounding RuP side-walls. For example, in (**2**), the fluorescence lifetime was determined to be 0.33 ns (Fig. 6) — compare this to the lifetimes of 2.3 ns and 0.89 ns seen in **ZnP** (**3**) and dimer (**8**), respectively.[12] Second, oxygen has no significant impact on the ZnP fluorescence, similar to what is shown in Fig. 5a. Third, the RuP phosphorescence (**1**: 32%; **2**: 25%), although notably smaller than in the **RuP** (**4**) reference, is higher by a factor 1.8 ± 0.1 relative to the corresponding (**8**) or (**9**) dimers. Interactions between the side-wall RuP groups may localize some of the triplet energy on the periphery rather than funnelling it quantitatively to the ZnP core. Fourth, phosphorescence lifetime measurements (*i.e.*, RuP) led to decay dynamics that were best analyzed by a double-exponential fit with values of 0.27 ns and 4.2 ns. Observation of the long-lived component supports our hypothesis of a locally excited state, which is localized on the side wall periphery. In phosphorescence lifetime measurements — conducted with the (**8**) and (**9**) dimers — only the short-lived component was seen. Finally, admission of oxygen led to a substantial quenching of the **RuP** emission, which most likely embraces on the long-lived, localized state of the side-wall RuP groups (see also Fig. 5b).[13,14]

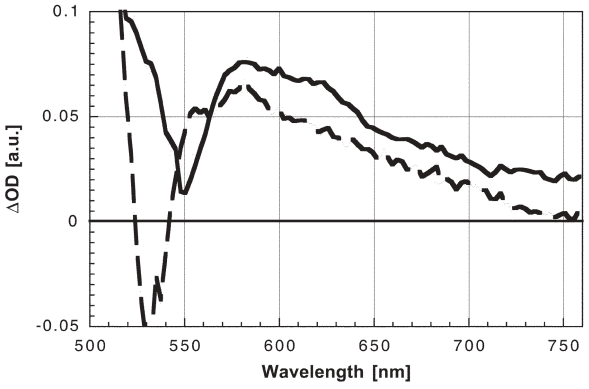

Fig. 7 Picosecond transient absorption spectrum (visible part) recorded at 25 ps (dashed line) and 1000 ps (solid line) upon flash photolysis of (**8**) (2×10^{-5} M) at 532 nm in deoxygenated toluene.

Differential absorption changes, recorded immediately after a 18 ps laser pulse of a toluene solution of (**1**) or (**2**), are identical to those summarized above for (**4**), (**8**) and (**9**): maxima at 370, 470, 590 and 870 nm and a minimum at 535 nm are clear attributes of ^{3}*(π–π*)RuP and point to the selective excitation of the ruthenium side-wall porphyrins (compare to Fig. 7). Instead of finding, however, the long-lived triplet excited state features of the aforementioned, with a lifetime of nearly 30 μs, the transient decays rather rapidly. In the near-infrared, the triplet deactivation is accompanied by the growth of a new absorption band at 860 nm — the ^{3}*(π–π*)ZnP fingerprint. In the case of (**2**), the potential triplet–triplet energy transfer takes place with a lifetime of 249 ps, while the underlying process at 393 ps is slightly slower for (**1**). The slower rates, seen for the 4-py isomer, can be attributed to the weaker overlap, relative to the 3-py isomer, between the π-system of the two porphyrins. In a first order approximation, this originates from the orthogonal positioning in (**1**), rather than tilted alignment in (**2**), of the two porphyrins with respect to each other.

On the nanosecond time scale the identity of the transient species detected is unambiguous. In particular, the 860 nm maximum is a clear attribute of the ^{3}*(π–π*)ZnP in the **ZnP** (**3**) reference. In addition, the triplet quantum yields, relative to the same **ZnP** (**3**) reference, are about 60% (**1**) and (**2**). This clearly documents the efficient energy funnelling between the different porphyrin moieties in both boxes.

Photochemistry of C$_{60}$–porphyrin box complexes. With the objective to link an electron acceptor, such as a 3-dimensional fullerene, to (**1**) and (**2**), a **C$_{60}$**-ligand was chosen bearing a pyridine functionality (**7**). The pyridine function is known to coordinate zinc centers in macrocyclic metalloporphyrins or metallophthalocyanines.[15] In principle, this could allow us to self-assemble a three-dimensional ensemble, constituted by the four side-wall chromophores (*i.e.*, RuP) the central chromophore (*i.e.*, ZnP) and possibly the coordinated electron acceptor (*i.e.*, **7**). This would mimic the two primary processes of photosynthesis: a sequence of unidirectional and efficient energy transfers from the side-wall RuP groups to the central ZnP followed by an intramolecular electron transfer to **7**.

The much stronger π-back bonding ruthenium center was, however, found to play a conflicting role in the formation and, moreover, in the stability of the (**1**) ensemble. Addition of various concentrations of **7**, led to a progressive increase of the porphyrin emission. In the intact box (**1**), the RuP phosphorescence is subject to a near quantitative quenching (*vide supra*). The reactivation of the emission can be taken as a sensitive measure for the complete and unexpected destruction of (**1**), by interfering with the fragile RuP-ZnP bonds.[16]

Photochemistry of C$_{60}$–porphyrin box complexes evolving from the excited ZnP. This led us to probe (**1**) and (**2**) with **C$_{60}$** in toluene. Most importantly, upon addition of various concentrations of **5** and **6**, no indication was given that would implicate the destruction of neither porphyrin box (*i.e.*, **1** and **2**).

Irradiation at 410 nm, the maximum of the RuP *Soret*-band, or 530 nm, the maximum of the RuP *Q*-band led to a nearly quantitative excitation of RuP and, as a direct consequence, the ZnP fluorescence is largely absent. Upon selecting 550 nm as the excitation wavelength, the opposite behavior was seen, namely, predominant ZnP fluorescence with only some residual amounts of RuP phosphorescence.

A real ZnP fluorescence still remains, allowing to probe the interactions between C_{60} and the central ZnP in (**1**) (5.8×10^{-6} M). To eliminate the residual RuP phosphorescence aerobic conditions were selected, which has no significant effects on the short-lived ZnP fluorescence. Addition of various concentrations of **5** or **6** ($0.4–1.6 \times 10^{-5}$ M) led to a concentration dependent quenching of the fluorescence associated with the ZnP (Fig. 8a). In particular, the maximal quenching is 12.5% at a fullerene concentration of 1.6×10^{-5} M, significantly larger than the ground state absorption of **5** or **6** at the excitation wavelength of 2.2%, relative to the porphyrin box absorption at 550 nm. Since the fluorescence lifetime of ZnP in (**1**) is short (0.33 ns), even a figure of 12.5% can be considered meaningful.

A parallel experiment with just the **ZnP** (**3**) reference, which exhibits a 7 times longer fluorescence lifetime (*i.e.*, 2.3 ns!), and the same $\mathbf{C_{60}}$ increments showed no noticeable decrease of the porphyrin emission at all. This leads us to conclude that in the (**1**) box, the orthogonal assembly of the ZnP and RuP moieties indeed facilitates embedding the fullerene core and, hence, helps to mediate a fast *intra*molecular quenching. Fitting the I/I_0 *versus* [$\mathbf{C_{60}}$] relationship to a previously developed procedure, a value of about 9650 ± 175 M^{-1} was obtained for the stability constant of $\mathbf{C_{60}}$–(**1**) in toluene.[17]

An independent set of experiments with (**2**) gave rise to a completely different picture. In fact, no appreciable fluorescence quenching was observed upon addition of the same increments of **5** or **6** to a toluene solution of (**2**) (Fig. 8b).

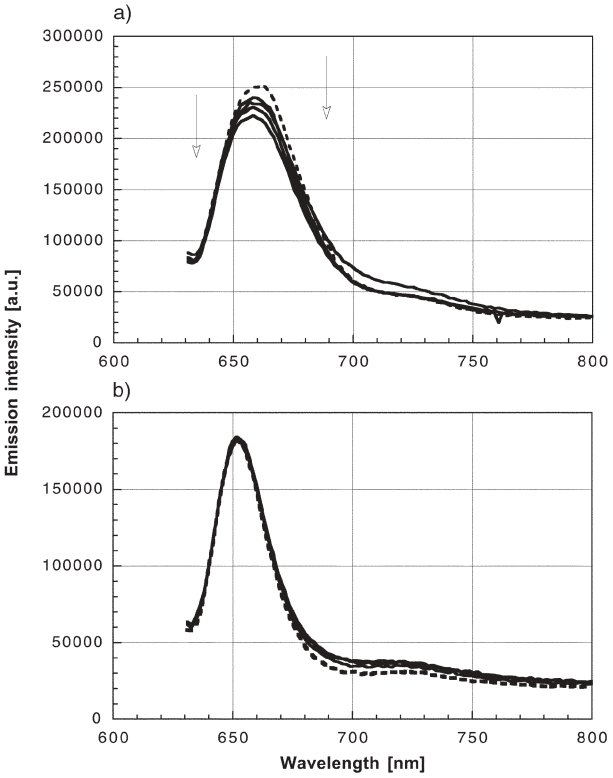

Fig. 8 Fluorescence spectra ($\lambda_{exc} = 550$ nm) of (a) (**1**) (5.8×10^{-6} M) and (b) (**2**) (5.8×10^{-6} M) in the presence of variable concentration of **5** ($0.4–1.6 \times 10^{-5}$ M) in oxygenated toluene at room temperature. Arrows indicate the decreased fluorescence quantum yields with increasing concentration of **5**.

Photochemistry of C_{60}–porphyrin box complexes evolving from the excited RuP. A different picture was found in an oxygen-free environment. The most striking observation is the much stronger emission of ^{3}*(π–π*)RuP, due to the absence of the triplet quencher (*vide supra*). Resembling effects were also seen upon lowering the temperature to 77 K of either an aerated or deaerated sample. In the case of aerated conditions, this behavior can be ascribed to the rigid matrix hindering the diffusion of molecular oxygen and, in turn, diminishing the triplet quenching.

In both scenarios, namely, at low temperature and under anaerobic working conditions, addition of **5** and **6** in concentrations ranging from 0.4 to 1.6×10^{-5} M led to a strong reactivation of the ^{3}*(π–π*)RuP emission. With the assumption that an efficient interplay exists between ZnP and RuP groups, the presence of **5** or **6** clearly perturbs the system. In the resulting $\mathbf{C_{60}}$–(**1**) complex, interactions between any of the porphyrins and $\mathbf{C_{60}}$ are expected to prevail and, in turn, to interfere with the *intra*molecular triplet–triplet energy transfer (*i.e.*, RuP → ZnP).

The low temperature experiments reveal that the overall enhancement is further accompanied by a concentration-dependent shift of the phosphorescence maxima to the red, from 715 nm (in the absence of **5**) to 721 nm (1.6×10^{-5} M of **5**). It is worthy of note that the low temperature emission of **RuP** (**4**) is located at 716 nm. The observed shifts lead to the premise that the red-shifted maxima evolve from an energetically low-lying state, which is governed by the mutual interaction between $\mathbf{C_{60}}$ and the side-wall RuP groups. At room temperature, a comparable trend has also been deduced, but due to significant broadening of the transitions the corresponding shift of 2 nm is rather moderate.[18,19]

To provide decisive evidence for the existence of strong $\mathbf{C_{60}}$–(**1**) interactions we probed (**1**) and (**2**) with variable $\mathbf{C_{60}}$ concentrations in time-resolved photolysis experiments following a 5 ns laser pulse (532 nm). Again the differential absorption spectra monitored in the blank runs (*i.e.*, (**1**) and (**2**) without $\mathbf{C_{60}}$) resemble the spectral features of the ^{3}*(π–π*)ZnP. Upon addition of variable concentrations **5** and **6**, the fullerene specific triplet–triplet maxima at 750 nm and 700 nm (*vide supra*), respectively were observed. Hereby, the intensity of the latter transitions, as shown in Fig. 9a, increased linearly with the $\mathbf{C_{60}}$ concentrations for (**1**).

Analyzing the kinetic time-profiles in details revealed that the $\mathbf{C_{60}}$ triplet formation is practically instantaneous, even at the lowest applied concentration (*i.e.*, 0.4×10^{-5} M). Considering a time resolution of 10 ns for our detection systems an *inter*molecular rate constant of 2.5×10^{13} M^{-1} s^{-1} would evolve for an energy transfer scenario. This estimate is more than three orders of magnitude higher than the diffusion-controlled limit for an *inter*molecular reaction in toluene, which is around 1.1×10^{10} M^{-1} s^{-1}. Consequently, this *inter*molecular pathway can be eliminated from the list of possible options.

Although the highest $\mathbf{C_{60}}$ concentration absorbs only 2.2% of the incoming photons at the 532 nm excitation wavelength, the $\mathbf{C_{60}}$ triplet quantum yield, relative to a blank (*i.e.*, highest $\mathbf{C_{60}}$ concentration without the porphyrin box) is 90% for (**1**). In the analogous (**2**), where the tilted alignment of the RuP groups do not allow $\mathbf{C_{60}}$ incorporation, the triplet quantum yield is only 23% (Fig. 9b). This clearly underlines that the efficient energy funnelling from the porphyrin box, either from the central ZnP or the four RuP side-walls, to the energy accepting fullerene is made possible by the geometry of the box.

Conclusions

In summary the current work documents, for the first time, that photochemical means can be used to probe the supramolecular interactions in a $\mathbf{C_{60}}$–rigid porphyrin system, promoted by a

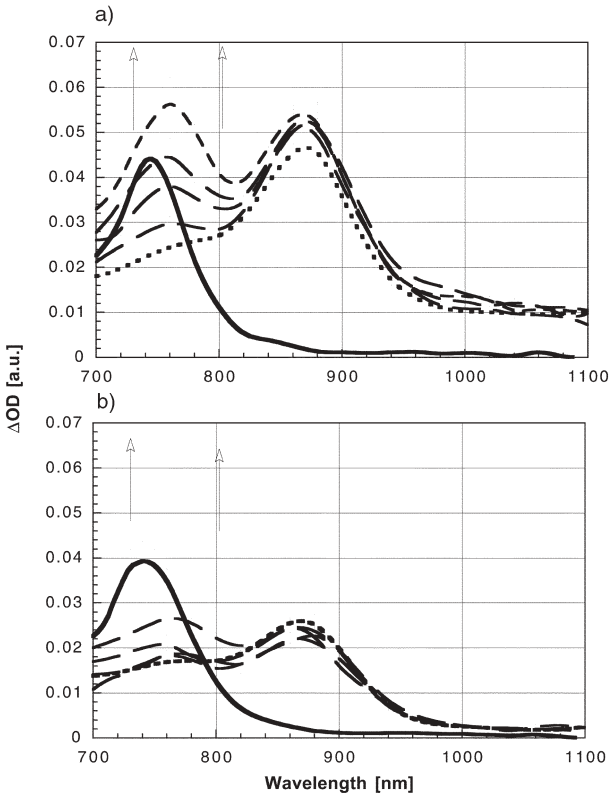

Fig. 9 Nanosecond transient absorption spectrum (near-infrared part) recorded at 50 ns upon flash photolysis of (a) (**1**) (5.8×10^{-6} M) and (b) (**2**) (5.8×10^{-6} M) in the presence of variable concentration of **5** ($0.4–1.6 \times 10^{-5}$ M) at 532 nm in deoxygenated toluene. Arrows indicate the increased triplet quantum yields with increasing concentration of **1**. The solid lines represent the spectra of the fullerene triplet probed without (**1**) and (**2**).

multi-point contact approach. In particular, the systematic variation of the **ZnP(4)-(RuP)$_4$** (**1**)/ **ZnP(3)-(RuP)$_4$** (**2**) geometry, namely, an open *versus* a congested box, facilitates or hinders the interactions with a three-dimensional **C_{60}** moiety. Our studies have mainly focused on the steady-state emission of the ZnP (*i.e.*, fluorescence) and the RuP (*i.e.*, phosphorescence) moieties. Conclusive evidence for the efficient communication is given by transient absorption spectroscopy, which reveals the nearly quantitative formation of the **C_{60}** triplet excited state. Generation of the latter state originates unambiguously from fast excited state transfer processes rather than from a direct excitation of the **C_{60}** moiety.

The association constants are notably weaker than the recently reported values for a porphyrin dimer,[8b] which are on the order of 10^6 M^{-1}. The difference in the association behavior can be rationalized in terms of different geometrical features: the flexible framework of the "cyclic-dimer" ensures perfect encapsulation of the fullerene sphere. In fact, X-ray crystallographic data for the C_{60}-"cyclic-dimer" complex reveal shortest zinc–carbon distances of 2.765 and 2.918 Å, notably shorter than the sum of the van der Waals radii (3.09 Å).[8b] In addition, the hexamethylene spacers are folded and the planarity of the porphyrin groups is slightly distorted to maximize the π-overlap with the convex C_{60} surface. When the flexibility was precluded, by using a rigid diacetylenic spacer instead of the hexamethylene spacer, no complex association was found at all.[8b]

Experimental section

Synthesis

The synthesis of the porphyrin complexes has already been reported.[9]

Modeling

Spartan version 4.1.2 runs on a Silicon Graphics SGI O2 R10000 workstation. Mopac (version 7) calculations and MOE (version 2001.01) energy minimizations and docking simulations were performed on a i686 Linux workstation. The complex pictures were produced by Tripos Sybyl 6.8 on the SGI O2 workstation.

The porphyrin (**1**) box structure was originally sketched with Spartan molecular modeling software and coarsely minimized with Sybyl force field in its Spartan implementation. The structure was then imported into MOE program for a further refinement by energy minimization in three steps with Merck force field (MMFF94).[20] In the first step, we used the Steepest Descent algorithm with an RMS gradient termination of 1000. In the second step the Conjugated Gradient algorithm was used with an RMS gradient termination of 100, whereas the last minimization was performed with a Truncated Newton algorithm with an RMS gradient termination set to 0.01. The partial charges on the porphyrin atoms were calculated by a semi-empirical quantum mechanics calculation using PM3 method by mopac software.

The docking simulation of the C_{60} into the porphyrin box was performed by MOE-dock program. The docking box around the porphyrin was designed to enclose only one half of the structure, since it is symmetrical and its dimensions was set to $55 \times 55 \times 35$ Å. The simulation included six cycles of a simulated annealing for each of 25 random starting conformations, with an initial temperature of 1000 K. The MMFF94 force field was used.

Photophysics

Picosecond laser flash photolysis experiments were carried out with 532-nm laser pulses from a mode-locked, Q-switched Quantel YG-501 DP Nd:YAG laser system (18 ps pulse width, 2–3 mJ $pulse^{-1}$). Nanosecond Laser Flash Photolysis experiments were performed with laser pulses from a Quanta-Ray CDR Nd:YAG system (532 nm, 6 ns pulse width) in a front face excitation geometry. The quantum yields of the triplet excited states (Φ) were determined by the triplet–triplet energy transfer method using β-carotene as an energy acceptor.

Fluorescence lifetimes were measured with a Laser Strope Fluorescence Lifetime Spectrometer (Photon Technology International) with 337 nm laser pulses from a nitrogen laser fiber-coupled to a lens-based T-formal sample compartment equipped with a stroboscopic detector. Details of the Laser Strobe systems are described on the manufacture's web site, http://www.pti-nj.com.

Emission spectra were recorded with a SLM 8100 Spectrofluorometer. The experiments were performed at room temperature or, alternatively, in a frozen matrix at 77 K. Each spectrum represents an average of at least 5 individual scans, and appropriate corrections were applied whenever necessary.

Acknowledgement

This work was carried out with partial support from the University of Trieste (Fondo 60%), MURST (PRIN 2000, MM03198284), CNR programme "Materiali Innovativi (legge 95/95)" and the Office of Basic Energy Sciences of the U.S. Department of Energy. This is document NDRL-4376 from the Notre Dame Radiation Laboratory.

References

1 (*a*) H. Anderson, C. Hunter and J. Sanders, *J. Chem. Soc., Chem. Commun.*, 1989, 226; (*b*) J. L. Sessler, B. Wang, S. L. Springs and C. T. Brown, in *Comprehensive Supramolecular Chemistry*, eds. J. L. Atwood, J. E. D. Davies, D. D. MacNicol, F. Vögtle, and Y. Murakami, Pergamon/Elsevier, Oxford, UK, 1996;

(*e*) M. D. Ward, *Chem. Soc. Rev.*, 1997, **26**, 365; (*d*) T. Hayashi and H. Ogoshi, *Chem. Soc. Rev.*, 1997, **26**, 355.
2 *The Photosynthetic Reaction Center*, ed. J. Deisenhofer and J. R. Norris, Academic Press, New York, 1993.
3 (*a*) F. Vögtle, *Supramolecular Chemistry*, Wiley, Chichester, 1991; (*b*) J. M. Lehn, Supramolecular Chemistry- Concepts and Perspectives, VCH, Weinheim, 1995; (*c*) J. W. Steed and J. L. Atwood, *Supramolecular Chemistry*, Wiley, Chichester, 2000.
4 *Electron Transfer in Chemistry* Vol. I–V, ed. V. Balzani, Wiley-VCH, Weinheim, 2001.
5 (*a*) *Comprehensive Supramolecular Chemistry* Vol. 1–10, eds. J. L. Atwood, J. E. D. Davies, D. D. MacNicol, F. Vögtle, and J.-M. Lehn, Pergamon/Elsevier, Oxford, UK, 1996; (*b*) L. F. Lindoy and I. M. Atkinson, *Self-Assembly in Supramolecular Systems*, Royal Society of Chemistry, Cambridge, UK, 2000.
6 (*a*) D. R. Evans, N. L. P. Fackler, Z. Xie, C. E. F. Rickard, P. D. W. Boyd and C. A. Reed, *J. Am. Chem. Soc.*, 1999, **121**, 8466; (*b*) P. D. W. Boyd, M. C. Hodgson, C. E. F. Rickard, A. G. Oliver, L. Chaker, P. J. Brothers, R. D. Bolskar, F. S. Tham and C. A. Reed, *J. Am. Chem. Soc.*, 1999, **121**, 10487; (*c*) M. M. Olmstead, D. A. Costa, K. Maitra, B. C. Noll, S. L. Phillips, P. M. van Calcar and A. L. Balch, *J. Am. Chem. Soc.*, 1999, **121**, 709; (*d*) T. Ishii, N. Aizawa, M. Yamashita, H. Matsuzaka, T. Kodama, K. Kikuchi, I. Ikemoto and Y. Iwasa, *J. Chem. Soc., Dalton Trans.*, 2000, 4407; (*e*) D. V. Konarev, I. S. Neretin, Y. L. Slovokhotov, E. I. Yudanova, N. V. Drichko, Y. M. Shul'ga, B. P. Tarasov, L. L. Gumanov, A. S. Batsanov, J. A. K. Howard and R. N. Lyubovskaya, *Chem. Eur. J.*, 2001, **7**, 2605.
7 (*a*) P. S. Baran, R. R. Monaco, A. U. Khan, D. I. Schuster and S. R. Wilson, *J. Am. Chem. Soc.*, 1997, **119**, 8363; (*b*) M. Kawaguchi, A. Ikeda, I. Hamachi and S. Shinkai, *Tetrahedron Lett.*, 1999, **40**, 8245; (*c*) D. I. Schuster, *Carbon*, 2000, **38**, 1607; (*d*) D. M. Guldi, C. Luo, M. Prato, A. Troisi, F. Zerbetto, M. Scheloske, E. Dietel, W. Bauer and A. Hirsch, *J. Am. Chem. Soc.*, 2001, **123**, 9166.
8 Examples of non-covalently linked porphyrin-fullerene ensembles (*a*) K. Tashiro, T. Aida, J.-Y. Zheng, K. Kinbara, K. Saigo, S. Sakamoto and K. Yamaguchi, *J. Am. Chem. Soc.*, 1999, **121**, 9477; (*b*) J.-Y. Zheng, K. Tashiro, Y. Hirabayashi, K. Kinbara, K. Saigo, T. Aida, S. Sakamoto and K. Yamaguchi, *Angew. Chem., Int. Ed.*, 2001, **40**, 1858; (*c*) D. Sun, F. S. Tham, C. A. Reed, L. Chaker, M. Burgess and P. D. W. Boyd, *J. Am. Chem. Soc.*, 2001, **123**, 10704.
9 (*a*) E. Alessio, M. Macchi, S. Heath and L. G. Marzilli, *Chem. Commun.*, 1996, 1411; (*b*) E. Alessio, S. Geremia, S. Mestroni, E. Iengo, I. Srnova and M. Slouf, *Inorg. Chem.*, 1999, **38**, 869; (*c*) E. Alessio, S. Geremia, S. Mestroni, I. Srnova, M. Slouf, T. Gianferrara and A. Prodi, *Inorg. Chem.*, 1999, **38**, 2527; (*d*) A. Prodi, M. T. Indelli, C. J. Kleverlaan, F. Scandola, E. Alessio, T. Gianferrara and L. G. Marzilli, *Chem. Eur. J.*, 1999, **5**, 2668.
10 (*a*) C. S. Foote, *Top. Curr. Chem.*, 1994, **169**, 347; (*b*) D. M. Guldi and M. Prato, *Acc. Chem. Res.*, 2000, **33**, 695.
11 Saturation of the toluene solutions with molecular oxygen led to a five-fold enhancement of the phosphorescence quenching.
12 Based on the substantial absorption of the RuP side-walls, ZnP fluorescence quantum yield measurements turned out to be unreliable.
13 Molecular oxygen had only an impact on the long-lived component.
14 An alternative rationale for the latter observation is that an equilibrium between the two triplet states ensures the reaction with oxygen.
15 (*a*) N. Armaroli, F. Diederich, L. Echegoyen, T. Habicher, L. Flamigni, G. Marconi and J. F. Nierengarten, *New J. Chem.*, 1999, 77; (*b*) F. D'Souza, G. R. Deviprasad, M. S. Rahman and J.-P. Choi, *Inorg. Chem.*, 1999, **38**, 2157; (*c*) T. Da Ros, M. Prato, D. M. Guldi, E. Alessio, M. Ruzzi and L. Pasimeni, *Chem. Commun.*, 1999, 635; (*d*) T. Da Ros, M. Prato, D. M. Guldi, M. Ruzzi and L. Pasimeni, *Chem. Eur. J.*, 2001, **7**, 816; (*e*) F. D'Souza, N. P. Rath, G. R. Deviprasad and M. E. Zandler, *Chem. Commun.*, 2001, 267 For a review, see F. Diederich and M. Gomez Lopez, *Chem. Soc. Rev.*, 1999, **28**, 263.
16 An alternative strategy to intensify the $\mathbf{C_{60}}$–(**1**) interactions implies applications of solvent conditions that might be unfavorable for dissolving $\mathbf{C_{60}}$, such as polar alcohols or acetonitrile. This is expected to provide the means to create a meaningful driving force for the hydrophobic $\mathbf{C_{60}}$ to nest within the likewise hydrophobic cavity of (**1**), resembling the basic concept used for the incorporation of, for example, a $\mathbf{C_{60}}$ guest into γ-cyclodextrine/calix[8]arene hosts. Again, a strongly attenuated RuP emission, even just upon addition of the neat solvent (*i.e.*, without $\mathbf{C_{60}}$) indicates the systematic destruction of (**1**). A possible rationale implies the insufficient stability of the Ru-N coordination bonds in these complexing solvents.
17 L. Famigni and M. B. Johnston, *New. J. Chem.*, 2001, **25**, 1368.
18 Extra evidence is given by experiments using 410 nm excitation in oxygenated systems. In the presence of oxygen (9.8×10^{-3} M) and **5** (up to 1.6×10^{-5} M), the RuP phosphorescence in (**1**) still increases despite the large excess of oxygen. The enhancement is, of course, by no means, as strong as seen in an oxygen-free solution. Based on the nearly diffusion-controlled dynamics, which govern the reaction of ^{3}*(π–π*)RuP with O_2, a reactivation of the RuP emission can only be rationalized, if an interaction, such as formation of an inclusion complex, with $\mathbf{C_{60}}$ is indeed quite strong.
19 Blank experiments implying an aerated sample of (**4**) or (**1**) and similar $\mathbf{C_{60}}$ concentrations did not result in any measurable changes at all.
20 T. A. Halgren, *J. Comp. Chem.*, 1996, **17**, 490.